JOURNAL OF COMPUTATIONAL PHYSICS 115, 515–523 (1994)

An Implicit–Explicit Hybrid Solver for a System of Stiff Kinetic Equations

PU SUN,* DAVID P. CHOCK, AND SANDRA L. WINKLER

Ford Research Laboratory, Ford Motor Company, P.O. Box 2053, MD-3083, Dearborn, Michigan 48121

Received June 7, 1993

A new stiff ordinary differential equation solver has been devised that separates the unknown variables into a fast group and a slow group. The fast variables are solved using the implicit backward-differentiation formulas but with a Jacobian of much smaller dimension than that of the original stiff system. The slow variables are solved using a simple explicit Adams–Bashforth scheme. The method, applied to a stiff atmospheric chemical system, yields an accuracy in the solution comparable to that of the commonly-used LSODE method at a relative tolerance level of 10^{-3} and an absolute tolerance level of 10^{-7} ppm, with one-third the execution time of LSODE. The method can be further fine-tuned to optimize its accuracy and execution time. As it is, the method should be an excellent candidate for the chemistry solver in air quality, combustion, and reactive flow models.

1. INTRODUCTION

Ordinary differential equations describing the time evolution of a system are considered stiff when the system contains processes of widely different time scales. These equations have a Jacobian matrix that has a wide range of eigenvalues. Many solvers are available that are applicable for specific types of stiff ordinary differential equations. The most general and commonly used solver is the Gear method [1] which is based on the backward-differentiation formulas. In particular, a Gear code, called the Livermore solver for ordinary differential equations (LSODE) that solves stiff and nonstiff systems [2, 3] has been a reliable solver against which other methods have often been compared.

In the Gear method, Newton's iteration procedure is necessary to achieve convergence of the solution without having to reduce the integration step size excessively. However, this procedure requires solving a linear system containing the Jacobian in its coefficient matrix. Although one can take advantage of the possible sparseness of the Jacobian matrix in specific applications, solving the linear system can be a time-consuming operation when the sparseness of the matrix cannot be presumed. To save computation time, the Jacobian matrix often is not updated at every integration step. In LSODE, for example, the Jacobian is updated at a default rate of every 20 integration steps at a potential sacrifice of some accuracy in the solution.

In a three-dimensional air quality model, both transport and chemistry of air pollutants are simulated. A time-splitting scheme is generally used to integrate the transport and chemistry steps in an alternating sequence. Depending on the method of choice, the chemistry step has to be reinitialized at every one or two time steps (Δt, typically 4 to 10 min).The atmospheric chemistry involves several tens of chemical species and some 80 to more than 100 chemical reactions. An example of the atmospheric chemistry model is the carbon-bond IV mechanism (CB4), which is used in the Urban Airshed Model recently released by the U.S. Environmental Protection Agency [4]. The system contains 38 chemical compounds and free radicals and 87 reaction steps. (The detailed chemical mechanism is described in [5]. More recent updates have been incorporated in the recently released Urban Airshed Model.) Thirty-two of the species are listed in Table I. The mechanism has a very wide range of reaction time scales. For example, from one of the initial conditions for the concentrations of 32 CB4 species displayed in Table I, the eigenvalue and eigenvector analysis of the Jacobian matrix for the daytime yields 32 eigenvalues whose orders of magnitude range from 10^{10} to 10^{-7}. Clearly, the stiffness ratio (the absolute maximum-to-minimum ratio of the real parts of all the eigenvalues of the Jacobian) in atmospheric chemistry is extremely large.

Because of the large number of species and reactions involved in atmospheric chemistry, the Jacobian has a high dimension, and a large number of the matrix elements are nonzero. Application of LSODE to solve the stiff chemical systems in each of the modeling grid cells is very time consuming. So far, many approximation schemes have been used to integrate the chemistry step that may reduce the computation time significantly. Two popular schemes are the quasi-steady-state approximation (see, e.g., [6]) and the hybrid scheme [7]. Both schemes avoid inverting the Jacobian matrix. One or both schemes have been compared to the Gear method in two recent studies [8, 9] using a limited number of initial conditions. Even though the approximations reduce the integration time significantly

* Also at the Institute for Mathematics and Its Applications, University of Minnesota, Minneapolis, MN 55455.

0021-9991/94 $6.00

TABLE I

Initial Concentrations (ppm)

	Low	High	Fixed					
NO	2×10^{-3}	6×10^{-2}	HONO	1×10^{-4}	OH	3.5×10^{-6}	CRES	1×10^{-5}
NO_2	2×10^{-3}	6×10^{-2}	H_2O_2	1×10^{-5}	C_2O_3	8.7×10^{-9}	PNA	1×10^{-5}
O_3	2×10^{-3}	3×10^{-1}	MGLY	1×10^{-3}	TO_2	6.6×10^{-9}	O^1D	1.6×10^{-12}
OLE	1×10^{-3}	3×10^{-2}	CO	5×10^{0}	CRO	1.3×10^{-11}	NO_3	1×10^{-5}
TOL	1×10^{-3}	1×10^{-2}	ETH	1×10^{-2}	HNO_3	1×10^{-5}	HO_2	1.7×10^{-7}
XYL	3×10^{-4}	1×10^{-2}	ISOP	1×10^{-2}	PAN	1×10^{-5}	ROR	5.9×10^{-11}
FORM	1×10^{-3}	1×10^{-2}	O	1.8×10^{-9}	OPEN	1×10^{-5}	XO_2	1.1×10^{-7}
ALD2	1×10^{-3}	2×10^{-2}	N_2O_5	8.1×10^{-9}	PAR	5×10^{-1}	XO_2N	4.6×10^{-8}

Note. Combining the low and high concentrations of species in the leftmost column generates a total of 256 initial conditions.

compared to LSODE for the cases tested, they sustain significantly reduced accuracy and lack of mass balance. To further reduce stiffness in the system, both schemes often invoke the steady-state assumption for the group of fastest-reacting species. However, there are two major problems with this approach. First, the nonlinear algebraic equations resulting from equating the first-order time derivatives of these stiff variables to zero may not be easy to solve, especially when several stiff variables are coupled together. Indeed, solving these algebraic equations can be very time consuming, defeating the original purpose of the steady-state assumption. Second, the reaction time scales vary among the "steady-state" species and with the integration time. The steady-state assumption ignores these variations and further contributes to reduced accuracy and lack of mass balance in the solutions. The impact of the resulting errors in the concentrations of the steady-state species is expected to propagate to the concentrations of non-steady-state species [10]. There is still a need to devise a method that is both accurate and fast for solving the highly stiff systems encountered in air quality modeling.

The LSODE uses the time-consuming implicit method for all species concentrations in a stiff system. A significant portion of the computation time is spent in solving the linear system in Newton's iterations. It would be advantageous if the dimension of the Jacobian matrix for a stiff-equation solver can be reduced. In this paper, a new implicit–explicit hybrid stiff-equation solver, to be called IEH, is proposed. This method partitions all the chemical species into two groups. The first group contains the fast-reacting species and is treated as a stiff system, while the second group contains the slow-reacting species which are considered nonstiff. The concentrations of the first group are solved using the accurate Gear method but with a Jacobian matrix of much smaller dimension, while the concentrations of the second group are solved with a fast explicit method. Since the number of equations requiring the implicit solver is now considerably reduced, the computation time for solving the whole system is expected to be significantly less than that of the solver that treats all species concentrations implicitly. Such a method should be particularly advantageous to air quality models and reactive flow models where complex chemical kinetic equations have to be solved for each of a large number of grid cells at each time step. Splitting the variables into two groups is not new. For example, Hofer [11] used a multistage one-step partially implicit approach that is second-order accurate, solving the slow variables (explicitly using midpoint rules) and fast variables (implicitly using the trapezoidal rule) alternately within one time step. Andrus [12] expressed the slow variables as given Taylor expansions in time in the equations for the fast variables, thus allowing the use of a large time step and avoiding constant updating of the solutions for the slow variables. Both methods are useful primarily for systems with few fast-varying variables. The method presented here, on the other hand, makes use of the highly accurate LSODE scheme for the fast variables and is applicable to large stiff systems such as the atmospheric chemical system.

The next section describes the methodology of the IEH method. Testing of the method with a large number of initial conditions will then be discussed to ascertain the robustness, accuracy, and computational efficiency of the method. A comparison of the new method with the commonly used LSODE and a more accurate version of LSODE, as applied to the atmospheric chemical model CB4, will be made. Comparison with other approximation schemes will be published elsewhere [13].

2. METHOD DESCRIPTION

The method is described as it is applied to the CB4 mechanism. If the system of stiff ordinary differential equations is written as

$$\frac{d\mathbf{C}}{dt} = \mathbf{f}(\mathbf{C}, t), \tag{1}$$

where $\mathbf{C}(t)$ is the concentration vector at time t, this equation can be rewritten as

$$\frac{d\mathbf{C}_F}{dt} = \mathbf{f}_F(\mathbf{C}_F, \mathbf{C}_S, t),$$
$$\frac{d\mathbf{C}_S}{dt} = \mathbf{f}_S(\mathbf{C}_F, \mathbf{C}_S, t), \quad (2)$$

where $\mathbf{C}_F$ and $\mathbf{C}_S$ are the fast-reacting and slow-reacting group concentrations, respectively. To partition the variables into fast and slow groups, we first inspected the temporal behavior of all the CB4 species concentrations using a limited set of realistic initial conditions in the full solver. The fast variables distinguish themselves by consistently displaying large, but short, transient behavior. There are "borderline" variables such as NO, NO_2, and O_3 which we grouped with the fast variables to help assure the solution accuracy. The resulting partition is consistent with the expectation from atmospheric chemistry. In general, free radicals have very low concentrations and large reaction rate constants. Their temporal behavior is very sensitive to slight changes in concentrations of more abundant species. They belong to the fast-variable group. On the other hand, concentrations of organic compounds tend to be higher and vary more slowly than those of free radicals. Consequently concentrations of organic compounds are expected to be grouped as slow variables. Concentrations of many oxides of nitrogen such as NO_3 and N_2O_5 can have large transient variations. Also, concentrations of NO, NO_2, and O_3 can have significant time dependence and play a very critical role in atmospheric chemistry. They are best classified as fast variables to assure their accuracy.

In all, 16 species of concentrations are classified as fast variables. They are NO, NO_2, O_3, PNA, O^1D, O, NO_3, N_2O_5, HO_2, OH, ROR, C_2O_3, XO_2, TO_2, XO_2N, and CRO. The remaining species concentrations constitute the slow variables: HONO, HNO_3, H_2O_2, FORM, ALD2, PAN, MGLY, OPEN, CO, PAR, OLE, ETH, TOL, XYL, CRES, and ISOP. (Note that six slow species concentrations, MEOH, ETOH, MTBE, NTR, SO_2, and SULF, are not listed because we set their initial values to zero. Either their initial concentrations are very low in the present atmosphere, or they have little influence on the ozone concentration (O_3), a major air pollutant. (Henceforth, we shall use the symbol like O_3 to represent either the species or its concentration.) At any rate, setting their initial concentrations to other than zero will not alter our conclusions. NTR is a product and a chain terminator. Its concentration will not be shown.) If the 16 fast variables are considered as a complete system, with the slow variables appearing in their time derivatives treated as "nonconstant coefficients," then the negative real parts of the eigenvalues of the resulting Jacobian matrix range from 10^0 to 10^{10}. The stiffness ratio of the fast variable system has been considerably reduced.

In (2), $\mathbf{C}_F$ will be integrated implicitly using the Jacobian matrix $\mathbf{J}_F = \partial\mathbf{f}_F/\partial\mathbf{C}_F$ in which $\mathbf{C}_S$ is treated as an independent set of parameters. Similarly, $\mathbf{C}_S$ will be integrated explicitly with $\mathbf{C}_F$ in $\mathbf{f}_S$ treated as an independent set of parameters. More specifically, given the initial condition at t_0, the implicit step based on LSODE for the fast-group species estimates h_0, which is then used to determine $\mathbf{C}_S(t_1)$ using the first-order explicit scheme. (Note that $t_{n+1} = t_n + h_n$, where h_n is an integration step, not to exceed the time step Δt, which is the time interval between two concentration outputs.) The result is then used in the implicit step to calculate $\mathbf{C}_F(t_1)$ and estimate h_1. But if h_0 should be readjusted to satisfy the local error tests of the implicit scheme, then $\mathbf{C}_S(t_1)$ will be redetermined, to be followed by a reevaluation of $C_F(t_1)$ and h_1. Otherwise, $C_S(t_2)$ will be calculated using the second-order Adams–Bashforth explicit scheme for $\mathbf{C}_S(t_{n+1})$,

$$\mathbf{C}_S(t_{n+1}) = \mathbf{C}_S(t_n) + h_n\left[\frac{h_n}{2h_{n-1}}(\mathbf{f}_S(t_n) - \mathbf{f}_S(t_{n-1})) + \mathbf{f}_S(t_n)\right], \quad (3)$$

where the time for $\mathbf{f}_S$ refers to the time for both $\mathbf{C}_S$ and $\mathbf{C}_F$ appearing in the equations. The solution, $\mathbf{C}_S(t_{n+1})$, is then used to solve for $\mathbf{C}_F(t_{n+1})$ and to estimate h_{n+1} in the implicit step, which in turn, together with $\mathbf{C}_F(t_n)$ are usd to determine $\mathbf{C}_S(t_{n+2})$. The same procedure is performed until $t_0 + \Delta t$ is reached. The second-order explicit scheme was selected after we found that the third- and fourth-order explicit schemes had led to only a minimal improvement in accuracy.

The LSODE is a highly versatile, multistep, fifth-order implicit scheme. The ultimate accuracy of the solutions is determined by the tolerance criteria set by the user. In the present approach, although $\mathbf{C}_S(t_{n+1})$ is used to integrate $\mathbf{C}_F$ from t_n to t_{n+1}, the integration step size h_n is determined by the fast-variable group. During the integration of $\mathbf{C}_F$, h_n is determined based on the existing values of $\mathbf{C}_S$ which may have to be updated. Consequently, h_n may be slightly reduced (compared to the LSODE case for the full system) to satisfy local error tests. However, this reduction of h_n also helps assure that $\mathbf{C}_S$ will have comparable accuracy as $\mathbf{C}_F$.

Assuming that n is the number of variables in LSODE. The LU decomposition scales as $n^3/3$ and the forward and backward substitutions scale as n^2. Reducing n from 38 to 16 would reduce the computation time to a factor of r^3 (=0.0746, r being $\frac{16}{38} = 0.421$) of the original for the LU decomposition and to a factor of r^2 (=0.1773) of the original for the forward and backward substitutions. The actual factors are expected to be greater. We found the factors of 0.14 and 0.26, respectively. The overall computation time for the atmospheric chemical system is reduced to about $\frac{1}{3}$ of the original (see below). Thus, the IEH can achieve a significant speedup while retaining high accuracy of the solutions.

In the present version of the IEH, the number of integration steps between two Jacobian updates in the fast-group species is set at 5 initially and reduced to 1 near the end of Δt. The IEH is to be compared with two LSODE methods for the full

set of species: one is the commonly used LSODE (denoted LSODE20), where the number of integration steps between two Jacobian updates is set at the default value of 20; the other is a slightly modified LSODE (denoted LSODE01), where the Jacobian is updated at every integration step. Clearly, LSODE01 is expected to be more accurate and more time consuming than LSODE20.

3. TEST CASES

Our comparison covers both the daytime and nighttime conditions. For the daytime case, the photolysis rate constants are set at their maximum values corresponding to the noontime condition in Los Angeles. For the nighttime case, the photolysis rates are set equal to zero. At night, even though the stiffness of the Jacobian will be reduced, sharp variations, such as a sharp drop essentially to zero in some species concentrations, often occur. Testing the IEH method for the nighttime condition is needed to assure the robustness in the applicability of the method. For all cases, the temperature is set at 310°K.

Since a solver may perform differently under different initial conditions, we establish 256 initial conditions by combining either a low or a high concentration from each of eight chemical species while holding other species' concentrations constant. Table I shows the initial concentrations used in the present study. The eight species with low and high concentrations are chosen for the following reasons: Both NO and NO_2 are key components in O_3 formation. They are also emitted by anthropogenic and natural sources. Therefore, they have a wide range of concentration values. Although not emitted, O_3 can vary widely in concentration and is the key species to be controlled. OLE, TOL, XYL, FORM, and ALD2 are reactive organic compounds that may have a rather wide range of concentration values. The species' extreme concentrations will impact the stiffness of the chemical system. Concentrations of other reactive organic species such as MGLY, ETH, ISOP, PAR, and CRES each could also have been assigned low and high initial values. But, with the exception of ISOP, the corresponding species are either not in abundant generally or relatively unreactive. More importantly, varying their initial concentrations in our test cases would most likely not introduce any new insights or modify the performance of the method revealed by changing the initial values of OLE, TOL, and XYL. (In fact, we did use a separate set of 256 initial conditions where HONO, MGLY, ETH, and ISOP were set at 1×10^{-5}, 1×10^{-5}, 1×10^{-3}, and 1×10^{-4} ppm, respectively. No significant change in the performance of the methods was found. In effect, 512 initial conditions have been tested in this comparison.) The range of the initial-concentration ratios of total organic species to NOx ($NO + NO_2$) is 4.9 to 208 ppmC/ppm. Our time integration is performed for one Δt, which is set at 6 min.

Three pairs of relative and absolute tolerances are used in our study. They are 1×10^{-3} and 1×10^{-7} ppm, 1×10^{-5} and 1×10^{-9} ppm, 1×10^{-7} and 1×10^{-11} ppm. They will be designated as high, intermediate, and low tolerances, respectively. These tolerances are used to test the convergence of the fast-reacting species' concentrations during the iteration process. Since the error tolerance in the LSODE is defined as the sum of the absolute tolerance and a term which is the product of the relative tolerance and the species concentration, a large difference between the two terms means that the smaller one will be ignored. Furthermore, the wide range of species concentrations, from 10^{-12} to 10^{-1} ppm initially, also makes it difficult to assure uniform accuracy for all species' concentrations. Species whose concentrations either are very low or drop substantially during the course of time integration may not be as accurately determined as those with high concentrations, although in general, high accuracy in the high-concentration species is accompanied by high accuracy in the low-concentration species.

4. RESULTS

We use LSODE01 with a relative and an absolute tolerance of 1×10^{-7} and 1×10^{-11} ppm, respectively, as the "exact" result against which other method–tolerance pairs are measured. The relative error, RE, at the end of one time step is given by the concentration difference between a method–tolerance pair and the "exact," divided by the "exact" concentration. Tables II and III show the averages (denoted Avg|RE|) and the maxima (denoted Max|RE|), respectively, of the absolute values of the relative errors for each species over the 256 initial conditions. The top 16 species are the fast-reacting species while the bottom 16 are the slow-reacting species. Only the high and intermediate tolerance cases are shown to conserve space. Let us first discuss the daytime results. For Avg|RE| in the high tolerance case, IEH, LSODE20, and LSODE01 yield results of comparable accuracy; the RE is typically 10^{-4}. (The relative differences among the solutions of the different methods are of the order of 10^{-4}. For intermediate tolerance, the RE is typically 10^{-5} for IEH and 10^{-6} for LSODE20 and LSODE01. (The relative differences among the results of IEH, LSODE20, and LSODE01 are 10^{-5}.) For low tolerance (not shown), the RE lowers to 10^{-6} for IEH and 10^{-8} to 10^{-7} for LSODE20. (The relative difference between the results of IEH and LSODE20 is 10^{-6}.) The Max|RE| is generally one order of magnitude higher and generally occurs when the species concentrations are either very low (as in the case of CRO) or below the tolerance levels.

For the nighttime case, both IEH and LSODE20 appear to have a higher Avg|RE| and Max|RE| for the fast-reacting species than their daytime counterpart. However, on closer inspection, the RE is not necessarily higher for all the initial conditions, but rather, the concentrations of some fast-reacting species, particularly NO, O_3, O^1D, O, NO_3, N_2O_5, and CRO, can approach zero rapidly for some initial conditions. (CRES of the second group, which forms CRO, can also decrease smoothly to practically zero under some initial conditions, re-

TABLE II

Average |RE| over the 256 Initial Conditions for All Species after One Time Step

	DAY						NIGHT					
	High Tolerance			Intermediate Tolerance			High Tolerance			Intermediate Tolerance		
Species	IEH	LSODE20	LSODE01	IEH	LSODE20	LSODE01	IEH	LSODE20	LSODE01	IEH	LSODE20	LSODE01
NO	1.36E-04	1.01E-04	7.40E-05	7.95E-06	1.61E-06	1.61E-06	1.26E-03	8.23E-03	7.02E-03	3.96E-04	1.10E-03	8.12E-04
NO2	1.71E-04	9.14E-05	7.60E-05	9.81E-06	1.15E-06	1.01E-06	1.08E-04	1.08E-04	1.35E-04	5.15E-06	8.96E-07	7.63E-07
O3	2.37E-04	1.09E-04	7.58E-05	1.03E-05	7.82E-07	7.01E-07	1.46E-01	8.81E-01	7.11E-01	1.12E-02	1.34E-02	1.07E-02
PNA	6.58E-04	3.40E-04	2.53E-04	4.91E-05	5.26E-06	7.07E-06	1.93E-03	1.14E-03	1.05E-03	8.47E-05	2.10E-05	2.15E-05
O1D	2.37E-04	1.09E-04	7.58E-05	1.03E-05	7.82E-07	7.01E-07	1.46E-01	8.81E-01	7.11E-01	1.12E-02	1.34E-02	1.07E-02
O	1.66E-04	7.28E-05	5.55E-05	9.66E-06	9.59E-07	8.39E-07	1.46E-01	8.66E-01	7.11E-01	1.12E-02	1.34E-02	1.07E-02
NO3	4.91E-04	1.81E-04	1.59E-04	2.37E-05	1.11E-06	1.85E-06	4.89E-02	9.16E+01	3.91E-01	5.77E-03	1.08E-02	5.46E-03
N2O5	8.21E-04	4.51E-04	4.15E-04	2.83E-05	5.43E-06	7.77E-06	9.36E-02	5.77E+00	4.20E-01	8.72E-03	3.21E-02	1.15E-02
HO2	5.62E-04	2.41E-04	1.88E-04	3.92E-05	3.83E-06	5.40E-06	1.91E-03	2.51E-03	9.83E-04	7.91E-05	1.99E-05	2.07E-05
OH	5.91E-04	2.39E-04	1.78E-04	3.53E-05	3.73E-06	5.03E-06	1.70E-03	1.74E-02	1.52E-03	7.42E-05	5.07E-05	2.45E-05
ROR	5.89E-04	2.39E-04	1.78E-04	3.49E-05	3.73E-06	5.03E-06	1.70E-03	1.75E-02	1.52E-03	7.41E-05	5.08E-05	2.45E-05
C2O3	6.18E-04	1.42E-04	1.21E-04	7.00E-05	1.44E-06	1.72E-06	1.06E-03	5.94E-03	9.07E-04	2.16E-04	1.87E-05	9.29E-06
XO2	6.07E-04	2.43E-04	1.81E-04	3.70E-05	3.67E-06	5.23E-06	1.65E-03	2.06E-03	1.37E-03	8.26E-05	2.78E-05	3.70E-05
TO2	5.73E-04	2.42E-04	1.76E-04	3.45E-05	3.68E-06	4.90E-06	1.69E-03	3.77E-03	1.49E-03	7.39E-05	3.81E-05	2.44E-05
XO2N	5.65E-04	5.83E-04	6.42E-04	3.21E-05	6.29E-06	6.58E-06	1.46E-03	6.20E-03	1.62E-03	1.36E-04	3.49E-05	3.76E-05
CRO	5.80E-03	1.53E-03	7.80E-04	2.05E-04	1.30E-05	3.21E-06	1.08E+01	2.25E-01	4.68E-03	5.12E-02	3.92E-03	9.96E-05
HONO	1.03E-03	1.14E-03	7.07E-04	1.53E-04	4.05E-06	3.05E-06	7.08E-04	2.64E-04	7.44E-05	1.28E-04	4.58E-06	2.49E-06
HNO3	1.64E-03	5.45E-04	4.79E-04	2.39E-04	2.37E-06	1.63E-06	2.48E-03	6.03E-04	6.03E-04	6.11E-04	1.17E-05	6.99E-06
H2O2	4.02E-04	2.68E-04	2.20E-04	1.04E-04	1.33E-06	1.33E-06	1.25E-03	7.33E-04	8.83E-04	3.53E-04	5.54E-06	5.59E-06
FORM	3.39E-04	6.93E-05	5.32E-05	5.56E-05	5.46E-07	6.08E-07	3.28E-04	3.38E-05	3.13E-05	5.37E-05	4.67E-07	6.27E-07
ALD2	2.27E-04	4.30E-05	3.12E-05	3.68E-05	3.41E-07	3.77E-07	1.68E-04	2.58E-05	2.21E-05	3.05E-05	3.39E-07	4.01E-07
PAN	1.06E-03	4.75E-04	3.86E-04	1.79E-04	3.03E-06	3.05E-06	1.65E-03	7.74E-04	8.67E-04	3.85E-04	7.32E-06	6.40E-06
MGLY	2.49E-04	7.45E-05	6.55E-05	4.19E-05	4.87E-07	5.13E-07	1.61E-04	3.08E-05	2.82E-05	2.73E-05	3.99E-07	3.48E-07
OPEN	5.97E-04	1.43E-04	9.78E-05	9.84E-05	1.62E-06	1.64E-06	7.41E-04	1.24E-04	1.10E-04	1.41E-04	2.41E-06	1.87E-06
CO	1.54E-07	3.02E-08	2.26E-08	2.62E-08	2.23E-10	2.47E-10	7.47E-08	1.13E-08	1.18E-08	1.28E-08	1.82E-10	1.63E-10
PAR	2.15E-06	4.22E-07	2.63E-07	3.64E-07	2.99E-09	3.37E-09	1.00E-06	1.50E-07	1.35E-07	1.87E-07	2.11E-09	2.46E-09
OLE	2.32E-05	5.32E-06	2.88E-06	3.96E-06	3.28E-08	3.66E-08	1.56E-05	2.23E-06	2.30E-06	3.59E-06	4.79E-08	4.54E-08
ETH	6.12E-05	1.61E-05	1.32E-05	1.03E-05	1.13E-07	1.20E-07	3.24E-05	7.04E-06	6.08E-06	5.48E-06	8.70E-08	6.97E-08
TOL	5.06E-06	1.03E-06	5.89E-07	8.41E-07	6.66E-09	7.40E-09	2.16E-06	3.33E-07	3.60E-07	3.74E-07	5.51E-09	4.86E-09
XYL	2.04E-05	4.28E-06	2.49E-06	3.41E-06	2.79E-08	3.12E-08	8.79E-06	1.35E-06	1.45E-06	1.52E-06	2.24E-08	1.98E-08
CRES	1.26E-03	9.79E-04	7.51E-04	1.78E-04	4.67E-06	1.98E-06	1.21E+01	1.44E-01	5.04E-03	4.33E-02	2.24E-04	1.01E-04
ISOP	7.87E-05	2.20E-05	1.74E-05	1.33E-05	1.44E-07	1.57E-07	6.26E-04	8.24E-05	7.86E-05	2.03E-04	2.02E-06	2.62E-06

TABLE III

Maximum |RE| over the 256 Initial Conditions for All Species after One Time Step

	DAY						NIGHT					
	High Tolerance			Intermediate Tolerance			High Tolerance			Intermediate Tolerance		
Species	IEH	LSODE20	LSODE01	IEH	LSODE20	LSODE01	IEH	LSODE20	LSODE01	IEH	LSODE20	LSODE01
NO	8.72E-04	9.67E-04	1.11E-03	6.93E-05	1.38E-05	1.28E-05	1.29E-02	6.73E-01	9.50E-02	1.25E-02	9.66E-02	1.42E-02
NO2	8.77E-04	6.46E-04	6.16E-04	5.77E-05	1.24E-05	1.14E-05	8.90E-04	1.19E-03	1.19E-03	1.90E-05	6.21E-06	8.16E-06
O3	1.86E-03	7.99E-04	7.35E-04	6.08E-05	1.02E-05	1.01E-05	1.36E+00	8.06E+00	4.25E+00	6.23E-02	7.21E-02	4.92E-02
PNA	2.67E-03	1.29E-03	1.10E-03	1.76E-04	2.27E-05	3.11E-05	2.10E-02	1.81E-02	2.02E-02	4.50E-04	2.54E-04	2.46E-04
O1D	1.86E-03	7.99E-04	7.35E-04	6.08E-05	1.02E-05	1.01E-05	1.36E+00	8.06E+00	4.25E+00	6.23E-02	7.21E-02	4.92E-02
O	8.91E-04	5.50E-04	5.05E-04	5.77E-05	9.96E-06	9.16E-06	1.36E+00	7.40E+00	4.25E+00	6.23E-02	7.21E-02	4.92E-02
NO3	4.10E-03	1.58E-03	1.19E-03	1.20E-04	1.20E-05	1.75E-05	7.49E-01	4.97E+03	3.87E+00	5.92E-02	1.65E-01	4.68E-02
N2O5	6.49E-03	4.02E-03	5.02E-03	1.52E-04	9.86E-05	9.00E-05	3.25E+00	1.97E+02	3.90E+00	1.17E-01	7.26E-01	1.49E-01
HO2	2.63E-03	1.18E-03	7.94E-04	1.37E-04	2.04E-05	2.76E-05	2.02E-02	7.58E-02	1.94E-02	4.35E-04	2.45E-04	2.37E-04
OH	3.82E-03	1.35E-03	7.17E-04	1.13E-04	1.81E-05	2.20E-05	2.00E-02	8.80E-01	1.94E-02	4.65E-04	2.10E-03	2.57E-04
ROR	3.81E-03	1.35E-03	7.18E-04	1.13E-04	1.81E-05	2.20E-05	2.00E-02	8.84E-01	1.94E-02	4.65E-04	2.10E-03	2.58E-04
C2O3	3.98E-03	9.74E-04	5.37E-04	2.25E-04	8.53E-06	5.81E-06	6.92E-03	2.98E-01	1.20E-02	8.09E-04	3.94E-04	6.42E-05
XO2	3.43E-03	1.81E-03	7.01E-04	1.29E-04	1.86E-05	2.47E-05	1.97E-02	3.64E-02	1.90E-02	4.40E-04	2.38E-04	2.31E-04
TO2	3.76E-03	1.35E-03	7.26E-04	1.14E-04	1.84E-05	2.22E-05	2.01E-02	1.46E-01	1.95E-02	4.61E-04	1.31E-03	2.57E-04
XO2N	2.80E-03	2.95E-03	4.10E-03	1.28E-04	3.35E-05	3.43E-05	1.11E-02	2.53E-01	2.02E-02	5.31E-04	4.25E-04	4.46E-04
CRO	9.27E-02	4.17E-02	8.15E-03	1.40E-03	5.12E-04	3.48E-05	3.38E+02	1.84E+01	1.08E-01	3.71E+00	1.71E-01	2.15E-03
HONO	2.31E-03	1.35E-02	6.23E-03	5.02E-04	2.64E-05	2.19E-05	4.83E-03	3.42E-03	4.47E-04	4.23E-04	4.02E-05	2.08E-05
HNO3	6.84E-03	4.27E-03	4.25E-03	6.81E-04	3.77E-05	9.14E-06	1.30E-02	3.97E-03	4.02E-03	2.42E-03	2.89E-04	7.45E-05
H2O2	2.30E-03	3.05E-03	2.44E-03	5.88E-04	9.62E-06	1.00E-05	8.11E-03	1.10E-02	1.11E-02	2.06E-03	4.73E-05	4.74E-05
FORM	1.84E-03	5.07E-04	4.55E-04	2.56E-04	5.64E-06	3.36E-06	2.95E-03	2.56E-04	2.77E-04	2.82E-04	4.02E-06	4.94E-06
ALD2	1.55E-03	4.42E-04	3.89E-04	2.28E-04	2.03E-06	2.74E-06	1.87E-03	2.67E-04	2.49E-04	1.91E-04	9.07E-06	1.15E-05
PAN	4.27E-03	2.92E-03	2.52E-03	3.90E-04	2.49E-05	1.48E-05	7.73E-03	1.02E-02	1.05E-02	1.45E-03	5.22E-05	7.07E-05
MGLY	8.91E-04	4.60E-04	4.60E-04	1.82E-04	3.18E-06	2.19E-06	8.44E-04	1.68E-04	1.69E-04	8.96E-05	5.65E-06	5.39E-06
OPEN	3.14E-03	8.12E-04	5.86E-04	3.47E-04	1.54E-05	1.38E-05	8.12E-03	1.96E-03	1.99E-03	6.90E-04	3.03E-05	2.38E-05
CO	5.05E-07	1.87E-07	1.63E-07	1.06E-07	2.00E-09	1.20E-09	3.42E-07	8.62E-08	8.68E-08	3.74E-08	1.80E-09	2.20E-09
PAR	8.77E-06	2.77E-06	1.96E-06	1.97E-06	3.31E-08	2.21E-08	5.33E-06	1.03E-06	9.71E-07	6.85E-07	2.78E-08	3.52E-08
OLE	7.01E-05	3.81E-05	2.57E-05	1.62E-05	2.44E-07	1.76E-07	4.59E-05	1.13E-05	1.13E-05	1.06E-05	4.41E-07	3.05E-07
ETH	1.82E-04	8.36E-05	8.52E-05	4.23E-05	7.89E-07	5.00E-07	1.40E-04	3.04E-05	3.05E-05	1.52E-05	1.53E-06	9.18E-07
TOL	1.59E-05	8.08E-06	5.75E-06	3.52E-06	5.73E-08	3.68E-08	9.48E-06	2.66E-06	2.68E-06	1.04E-06	5.51E-08	6.97E-08
XYL	6.32E-05	3.04E-05	2.35E-05	1.45E-05	2.35E-07	1.53E-07	3.85E-05	1.05E-05	1.05E-05	4.21E-06	2.21E-07	2.80E-07
CRES	7.25E-03	1.37E-02	7.82E-03	9.18E-04	4.88E-05	3.52E-05	3.25E+02	9.12E+00	1.09E-01	3.68E+00	1.59E-02	2.14E-03
ISOP	2.52E-04	1.45E-04	1.49E-04	6.00E-05	8.94E-07	6.77E-07	2.86E-03	6.65E-04	3.31E-04	7.16E-04	2.27E-05	1.48E-05

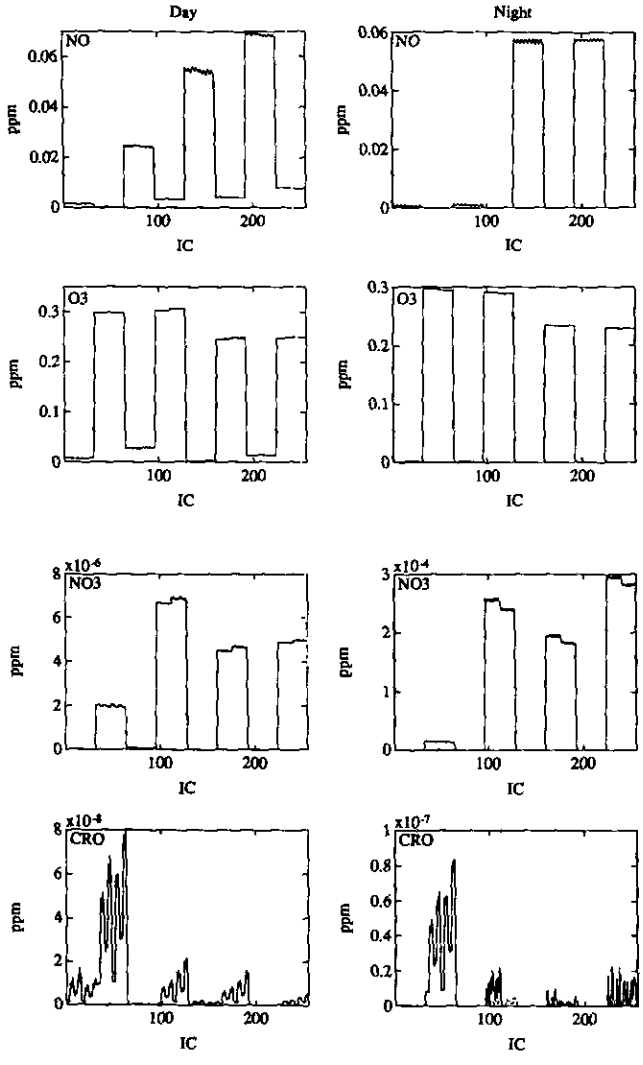

FIG. 1. The concentrations (ppm) for NO, O_3, NO_3, and CRO after one Δt daytime (left) simulation and one nighttime (right) simulation. In each plot, the solid line is the IEH result under high error tolerance; the dotted line is the "exact" result. They coincide almost fully. The abscissa represents the 256 initial conditions whose arrangement is akin to an increasing 8-digit binary number with the left-to-right order of the digit being identical to the top-to-bottom order of the eight species with two concentration levels in Table I: 0 (or *l*) = low and 1 (or *h*) = high.

sulting in a relatively large |RE|.) Although the IEH method and LSODE20 track the species' temporal behavior very well even in these cases, their RE becomes unreliable, and the Avg |RE| can therefore be inflated because the denominators are essentially zero or are close to or below the tolerance limit.

Figure 1 shows the concentrations of NO, O_3, NO_3, and CRO after one Δt each in the daytime (left) and nighttime (right) simulations. The behavior of O^1D and O is similar to O_3, while that of N_2O_5 is similar to NO_3. Therefore, they are not included in the figure. (No slow-reacting species are displayed because their temporal variation is smooth. CRES has a high |RE| only under the conditions of a very small denominator.) The abscissa of Fig. 1 corresponds to the 256 initial conditions, representing all combinations of the low and high initial concentrations of the eight species shown in Table I. Each initial condition is akin to an eight-digit binary number with the order of the digit from left to right being the same as that of the species from top to bottom in the table. The arrangement of the initial conditions in the abscissa from left to right is identical to an increasing eight-digit binary number where zero and one represent the low and high concentrations of a given species, respectively. Thus the left half and the right half of the abscissa correspond to the low and high initial NO values, respectively. The first and third quarters have the low initial NO_2 concentration while the second and fourth quarters have the high one, and so on. Each plot in Fig. 1 contains two lines, a solid line representing the solutions of the IEH method under high error tolerance and a dotted line representing the solutions of the "exact" method (LSODE01 under low error tolerance). The lines are indistinguishable from each other for both the daytime and nighttime simulations, with a small exception in the nighttime simulation of CRO. Since the nighttime simulations of these species under high error tolerance represent potentially the least accurate of all our simulations, the result in Fig. 1 is certainly encouraging. The nighttime runs also show bands of essentially zero concentrations for these species. The high |RE| regions of the species coincide with these bands. For O_3 and NO_3 (similarly for O^1D, O, and N_2O_5), and CRO, these bands correspond to the low-O_3 initial conditions. For NO, the low- or zero-concentration bands occur under low-NO or high-O_3 initial conditions. Figures 2 and 3 show the temporal behavior of NO, O_3, NO_3, and CRO concentrations in one Δt for two initial conditions in the daytime and nighttime simulations, respectively. The two initial conditions are *hllllhl* and *hhhllllh*, where *h* and *l* stand for high and low concentrations, respectively. Again, there are two lines in each plot, a solid line representing the IEH result under high error tolerance and a dotted line representing the "exact" result under low error tolerance. The time interval per concentration output is 12 s. For NO_3 under *hllllhl*, the concentration drop occurs in much less than 12 s. The figures show the very different behavior of the concentrations between daytime and nighttime and the transient nature of some of the species. They further show the excellent agreement between the high tolerance IEH results and the low tolerance "exact" results. This is true even for a CRO concentration as low as 10^{-10} ppm. One can conclude that the high |RE| in the IEH and LSODE20 methods in some instances is not due to any significant decrease in accuracy, but rather, a less reliable |RE| itself because of the small denominator. More importantly, the impact of this perceived high |RE| on the time integration of all species concentrations is insignificant.

Figures 4a and b show the execution times for the daytime and nighttime cases, respectively, for one 6-min time step using the IEH method as well as those using LSODE20 and LSODE01 relative to the IEH method of the same tolerance levels. The computation was carried out on a Kubota Pacific Titan 3000 Computer. The average execution times for the daytime condi-

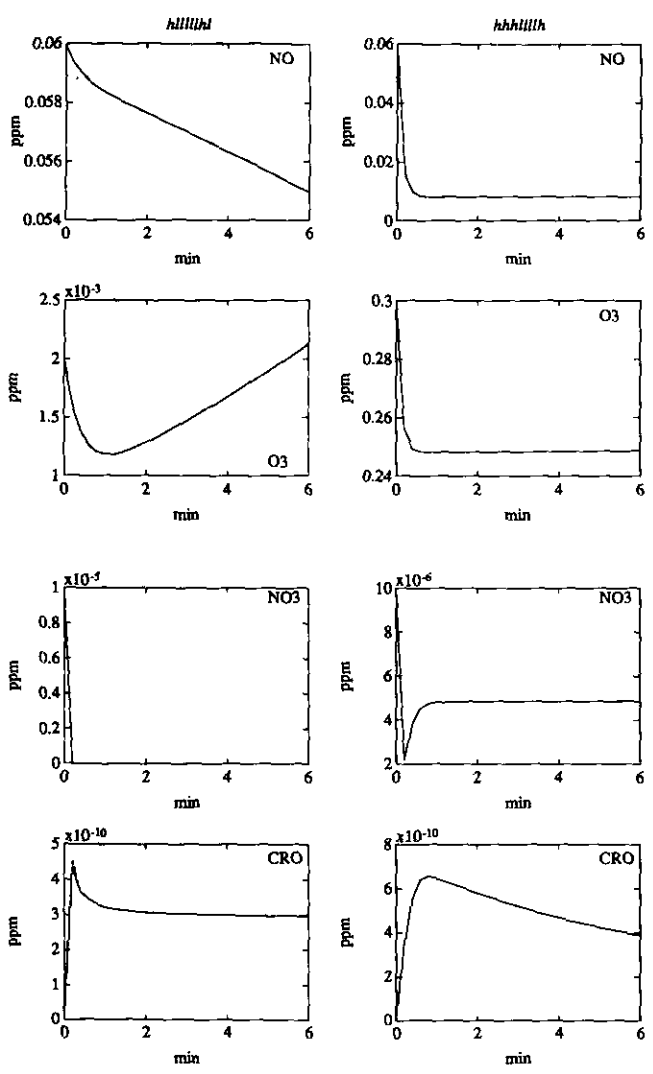

FIG. 2. The temporal behavior of NO, O_3, NO_3, and CRO concentrations (ppm) in one Δt (6 min) for two initial conditions in the daytime simulation. The two initial conditions are *hlllllhl*, and *hhhllllh*, where *h* and *l* stand for high and low concentrations, respectively, of the eight species shown in Table I. In each plot, the solid line is the IEH result under high error tolerance and the dotted line is the "exact" result. The time interval per concentration output is 12 s.

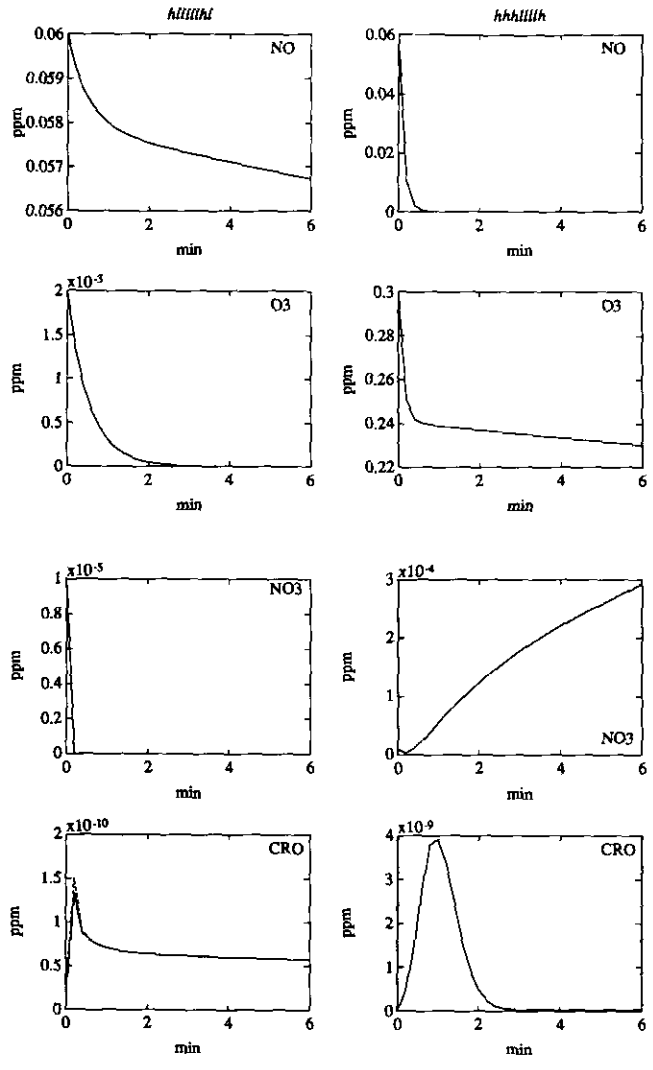

FIG. 3. Same as Fig. 2, except for the nighttime simulation.

tion over the 256 initial conditions with the IEH method are 0.090 s, 0.201 s, and 0.382 s, for the high, intermediate, and low tolerance levels, respectively. For the same tolerance levels, LSODE20 requires 3.2, 2.8, and 2.8 times the execution times of the IEH method, while LSODE01 requires 7.7, 8.4, and 8.1 times, respectively. For the nighttime condition, the execution times with the IEH method are 0.122, 0.221 s, and 0.399 s for the high, intermediate, and low tolerance levels, respectively. For the same tolerance levels, LSODE20 requires 2.5, 2.7, and 2.7 times the execution times of the IEH method, while LSODE01 requires 6.2, 7.7, and 8.0 times, respectively.

We have also separately tested the IEH method using 15 as the number of integration steps between two Jacobian updates for the daytime condition. In general, the accuracies are slightly lower than the IEH method reported above while the execution times are 0.096 s, 0.188 s, and 0.359 s for the high, intermediate, and low tolerance levels, respectively.

The nitrogen mass balance of the IEH method is found, as expected, to be in excellent agreement with the "exact" results for both the daytime and nighttime conditions. Note, however, that the CB4 mechanism itself allows for a gradual loss of the nitrogen mass in some chain-terminating steps.

5. CONCLUSIONS

From the results presented above, we see that by classifying the variables of a highly stiff system into fast and slow groups, and by solving the fast variables implicitly using the accurate backward-differentiation formulas and the slow variables explic-

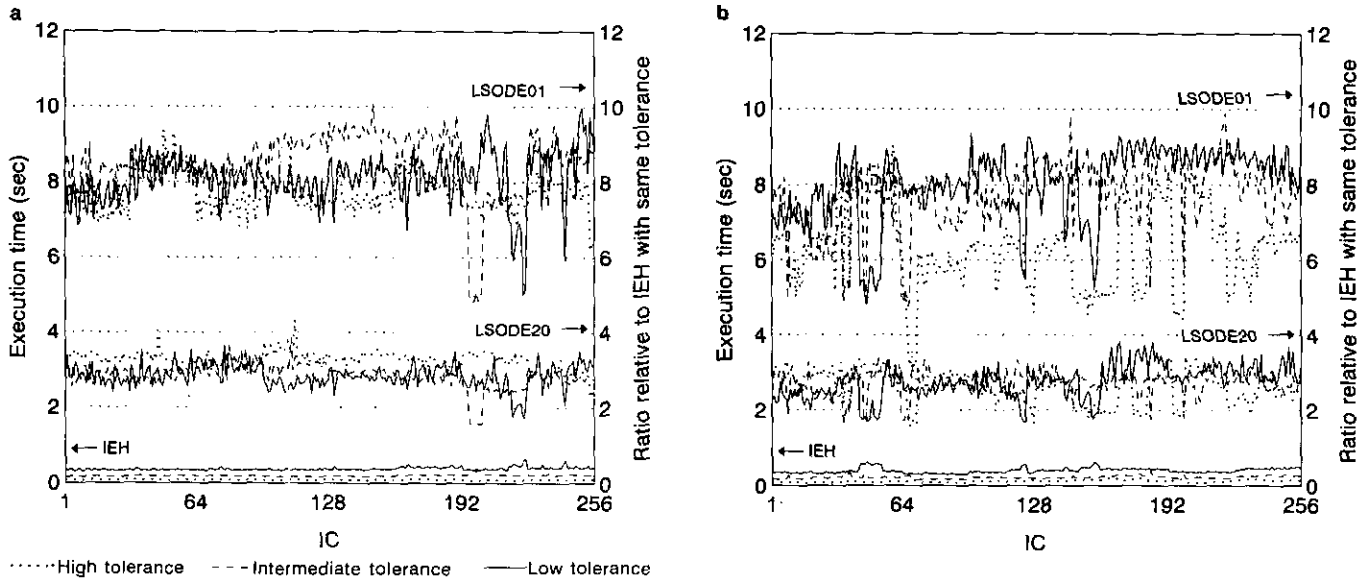

FIG. 4. The execution times for the daytime case (a) and the nighttime case (b) for one 6-min time step using the IEH method (left scale) and those using LSODE20 and LSODE01 relative to the IEH method of the same tolerance levels (right scale).

itly, we can achieve, in our application to atmospheric chemistry, an accuracy in the solution that is comparable to the commonly used LSODE at a relative tolerance level of 10^{-3} and an absolute tolerance level of 10^{-7} (pppm), with one-third the execution time of LSODE. In our atmospheric chemistry application, the new method is robust for a wide range of initial conditions and for a substantial variation in some rate constants due to a shift in, say, the daytime and nighttime conditions. The accuracy and execution time of the method can be further adjusted or optimized by (1) readjusting the grouping of fast and slow variables to further reduce the size of the Jacobian matrix for the fast variables, (2) adjusting the frequency of the Jacobian update for the fast variables either to improve accuracy or to save computation time, (3) introducing some steady-state variables that are simple to solve to further reduce the size of the Jacobian matrix without causing a significant mass imbalance. These options will be considered in a separate study. As it is, the method is significantly more accurate, at a comparable speed, than the chemistry solvers used in existing air quality models. This method is also useful in combustion and reactive-flow models, where repeated applications of a stiff-equation solver is required.

REFERENCES

1. C. W. Gear, *Numerical Initial Value Problems in Ordinary Differential Equations* (Prentice–Hall, Englewood Cliffs, NJ, 1971).
2. A. C. Hindmarsh, *ACM-SIGNUM Newsletter* **15**(4), 10 (1980).
3. A. C. Hindmarsh, "ODEPACK, a Systematized Collection of ODE Solvers," in *Numerical Methods for Scientific Computation*, Vol. 55, edited by R. S. Stepleman (North-Holland, New York, 1983).
4. U.S. Environmental Protection Agency, Urban Airshed Model Version 6.20, DATED 920825, Resarch Triangle Park, NC, 1993.
5. M. W. Gery, G. Z. Whitten, J. P. Killus, and M. C. Dodge, *J. Geophys. Res.* **94**, 12925 (1989).
6. E. Hesstvedt, Ø. Hov, and I. S. A. Isaksen, *Int. J. Chem. Kinet.* **10**, 971 (1978).
7. T. R. Young and J. P. Boris, *J. Phys. Chem.* **81**, 2424 (1977).
8. D. S. Shieh, Y. Chang, and G. R. Carmichael, *Environ. Software* **3**, 28 (1988).
9. M. T. Odman, N. Kumar, and A. G. Russell, *Atmos. Environ.* **A26**, 1783 (1992).
10. R. J. Gelinas, *J. Comput. Phys.* **9**, 222 (1972)
11. E. Hofer, *SIAM J. Numer. Anal.* **13**, 645 (1976).
12. J. F. Andrus, *SIAM J. Numer. Anal.* **16**, 605 (1979).
13. D. P. Chock, S. L. Winkler, and P. Sun, *Environ. Sci. Technol.*, **28**, 1882 (1994).